# Nonlinear thermal effects in ballistic electron devices

**Professor Heiner Linke**

**Lund University**
**Division of Solid State Physics**
**Box 118**
**Lund 22100  Sweden**

Report Date: March 2013

Final Report from 01 October 2011 to 31 December 2012

**Air Force Research Laboratory**
**Air Force Office of Scientific Research**
**European Office of Aerospace Research and Development**
**Unit 4515 Box 14, APO AE 09421**

| REPORT DOCUMENTATION PAGE | Form Approved OMB No. 0704-0188 |
|---|---|

Public reporting burden for this collection of information is estimated to average 1 hour per response, including the time for reviewing instructions, searching existing data sources, gathering and maintaining the data needed, and completing and reviewing the collection of information. Send comments regarding this burden estimate or any other aspect of this collection of information, including suggestions for reducing the burden, to Department of Defense, Washington Headquarters Services, Directorate for Information Operations and Reports (0704-0188), 1215 Jefferson Davis Highway, Suite 1204, Arlington, VA 22202-4302. Respondents should be aware that notwithstanding any other provision of law, no person shall be subject to any penalty for failing to comply with a collection of information if it does not display a currently valid OMB control number. **PLEASE DO NOT RETURN YOUR FORM TO THE ABOVE ADDRESS.**

| 1. REPORT DATE *(DD-MM-YYYY)* <br> 06 March 2013 | 2. REPORT TYPE <br> Final Report | 3. DATES COVERED *(From – To)* <br> 1 October 2011 – 31 December 2012 | |
|---|---|---|---|
| **4. TITLE AND SUBTITLE** <br><br> **Nonlinear thermal effects in ballistic electron devices** | | **5a. CONTRACT NUMBER** <br><br> **FA8655-11-1-3037** | |
| | | **5b. GRANT NUMBER** <br><br> **Grant 11-3037** | |
| | | **5c. PROGRAM ELEMENT NUMBER** <br><br> 61102F | |
| **6. AUTHOR(S)** <br><br> **Professor Heiner Linke** | | **5d. PROJECT NUMBER** | |
| | | **5d. TASK NUMBER** | |
| | | **5e. WORK UNIT NUMBER** | |
| **7. PERFORMING ORGANIZATION NAME(S) AND ADDRESS(ES)** <br> Lund University <br> Division of Solid State Physics <br> Box 118 <br> Lund 22100  Sweden | | **8. PERFORMING ORGANIZATION REPORT NUMBER** <br><br> N/A | |
| **9. SPONSORING/MONITORING AGENCY NAME(S) AND ADDRESS(ES)** <br><br> EOARD <br> Unit 4515 BOX 14 <br> APO AE 09421 | | **10. SPONSOR/MONITOR'S ACRONYM(S)** <br><br> AFRL/AFOSR/IOE (EOARD) | |
| | | **11. SPONSOR/MONITOR'S REPORT NUMBER(S)** <br><br> **AFRL-AFOSR-UK-TR-2013-0004** | |

**12. DISTRIBUTION/AVAILABILITY STATEMENT**

Approved for public release; distribution is unlimited.  (approval given by local Public Affairs Office)

**13. SUPPLEMENTARY NOTES**

**14. ABSTRACT**
Our results have shown that the transverse thermopower of the four-terminal junction with a central scatterer is very sensitive to the symmetry of the four QPC transmissions functions. We have shown that as a first order conceptual model, the four-terminal junction can be thought of as two pairs of QPCs, one left and one right. This model is capable of describing both the observed sign change in the transverse thermopower upon reversal of the thermal gradient, as well as the observed nonlinear effects in the transverse thermopowers. To fully take all four terminals into account, we have put forth a multi-terminal thermoelectric scattering theory, which we have used to extract the applied temperature increase as well as the effective transverse thermopower. Finally, we have experimentally demonstrated the fundamental magnetic-field symmetries of thermoelectric transport coefficients under thermal and electrical biases. We have also shown that these symmetries tend to decrease with increasing thermal bias. From our experiments we cannot conclude whether this symmetry breaking is due to a heating effect (for example the destruction of phase coherence due to inelastic scattering) or due to a nonlinear effect.

**15. SUBJECT TERMS**

EOARD, Thermophysics, thermoelectric, nano

| 16. SECURITY CLASSIFICATION OF: | | | 17. LIMITATION OF ABSTRACT | 18, NUMBER OF PAGES | 19a. NAME OF RESPONSIBLE PERSON <br> Kevin Bollino, Lt Col, USAF |
|---|---|---|---|---|---|
| **a. REPORT** <br> UNCLAS | **b. ABSTRACT** <br> UNCLAS | **c. THIS PAGE** <br> UNCLAS | SAR | 15 | **19b. TELEPHONE NUMBER** *(Include area code)* <br> +44 (0)1895 616163 |

**Standard Form 298** (Rev. 8/98)
Prescribed by ANSI Std. Z39-18

AIR FORCE OFFICE OF SCIENTIFIC RESEARCH
EUROPEAN OFFICE OFAEROSPACE RESEARCH AND DEVELOPMENT (EOARD)
**FINAL REPORT**
AFOSR-BAA-2010-1

20 December, 2012

# Nonlinear thermal effects in ballistic electron devices

| | |
|---|---|
| Principal Investigator: | Heiner Linke<br>The Nanometer Structure Consortium at Lund University<br>(nmC@LU) |
| Program Officer: | Dr. Kevin Bollino, EOARD, London |
| Award Number: | **FA8655-11-1-3037** |
| Institution: | Lund University, Sweden |
| Type of business: | Educational |
| Start date | 1 October, 2011 |
| Place of performance: | Division of Solid State Physics, Lund University, Sweden |
| Period of Award: | 1 October, 2011 – 30 September, 2012 |
| Period of Report: | until 30 September, 2012 |

| Technical Point of Contact: | Administrative Point of Contact |
|---|---|
| Prof. Linke, Heiner | Dr. Löfgren, Anneli |
| Division of Solid State Physics | Division of Solid State Physics |
| Lund University | Lund University |
| Box 118 | Box 118 |
| S – 22100 Lund | S – 22100 Lund |
| Sweden | Sweden |
| Ph: +46 70 414 0245 | Ph: +46 46 222 84 99 |
| Email: **Heiner.Linke@ftf.lth.se** | Email: **Anneli.Lofgren@ftf.lth.se** |

**Final Report for:**

Dr. Kevin Bollino

European Office of Aerospace R&D (EOARD), U.S. Air Force Research Laboratories

## Table of Contents

## A. Summary

To date, essentially all thermal and thermoelectric materials and devices are based on linear-response phenomena, where the effect (for example flow of heat or charge) is proportional to the driving force (a thermal or electric bias). This is in contrast to electronic devices, where the use of nonlinear elements, such as diodes, is widespread and enables key functionalities.

This report addresses ***thermal phenomena in nonlinear response***, with the goal to explore fundamentally new effects and functionalities that may enable game-changing, novel devices, and enhanced performance.

Electrons in semiconductor devices with sufficiently small (submicron) features move on straight trajectories (ballistically) between device boundaries, and electronic properties are therefore determined by the device symmetry. In this highly controllable system we have observed transverse thermoelectric effects in multi-terminal devices, and we have developed a scattering-matrix theory that explains these effects. Specifically, using this theory, we can predict the magnitude and direction of the transverse thermoelectric effect based on (nonlinear) electric characterization of the device. In other words, we now understand this system sufficiently well that we can predict its response to a *thermal* bias from measurements using an *electric* bias alone. We have thus established a framework for the targeted development of novel functional materials and devices based on nonlinear thermal phenomena.

The insights gained may be applicable not only to electronic systems, but also to heat flow carried by phonons in thermal devices. Military applications of rectified heat flow include solid-state refrigerators for FIR detectors (reduction of parasitic back flow of heat), and thermal management in high-power electronics.

## B. Introduction

### B.1. Background: New functionality in the nonlinear response regime

The functionalities of essentially all current applications of thermoelectricity and of thermal management are well described within linear response theory: Ohm's Law ($I = GV$) for charge current, Fourier's Law ($dQ/dt = K\Delta T$) for thermal conduction.

In the nonlinear regime, the higher terms in the following expansions become important:

$$I = GV + G_2 V^2 + G_3 V^3 + \ldots$$

$$dQ/dt = K\Delta T + K_2\Delta T^2 + K_3\Delta T^3$$

Current significant progress in nanostructured materials offers strong motivation to explore nonlinear thermal phenomena. First, on length scales shorter than the characteristic energy relaxation lengths of electrons and/or phonons, nonlinear effects (the breakdown of Fourier's Law) are very likely because the energy of electrons and/or phonons is no longer controlled by the temperature of the bath, but by the applied bias. Second, the ability to structure materials on the nanoscale with very high precision can be used to control the material's symmetry, enabling the control of, for example, rectifying phenomena.

New functionality is possible in this regime. For example, the second term in each equation above signifies rectifying effects, because this term enhances the current for one sign of the bias, and reduces it for the opposite sign.

### B.2. Motivation: Enabling novel functionalities and enhanced performance

The ability to control nonlinear thermal behavior would enable a number of novel functionalities and applications, as illustrated in the following examples:

> ***Example 1: Rectified heat flow in Peltier coolers, or in thermal management.*** In Peltier coolers, an applied electric current removes heat from a material, such that it can be cooled below ambient temperature. The performance of Peltier coolers is limited by the backflow of heat, in a direction opposite to that of the electric current. A nonlinear material in which electrons move easily in the direction of the current, but have a low

mobility in the direction of the heat backflow, could have significantly enhanced performance. *To date, thermal rectification has been demonstrated at some heterostructure interfaces but, to our knowledge, no functional, nanostructured material with this property has been designed.*

***Example 2: Transverse thermoelectrics.*** Also the performance of thermoelectric power generators is limited by undesired heat flow, but in this case electric current and parasitic heat flow are in the same directions. One relatively unexplored possibility is to *geometrically* decouple charge and heat flow, by using transverse thermoelectric effects, where the charge flow is perpendicular to the applied thermal gradient. Such effects can be induced in asymmetric nanostructures, potentially enabling the design of functional TE materials with enhanced performance.

Here, we report our research progress on the physical mechanisms underlying nonlinear thermal effects in a highly controlled experimental system that is amenable to the development and test of a rigorous theoretical framework.

## C. Methods, Assumptions, and Procedures

### C.1. Device Fabrication

Our experiments were carried out on two-dimensional electron gas (2DEG) devices embedded in InGaAs/InP heterostructure wafers. These heterostructures are grown on the surface of InP wafers at Lund University using metal organic vapor phase epitaxy. The composition of the heterostructure is shown in Fig. 1(a), the details of which are covered in Refs. 2-4. Wafers grown in this material and manner are nearly perfectly flat, offer high electron mobilities ($\mu_e > 10^5$ cm$^2$/Vs) [2,3], and can be chemically etched without the risk of surface oxidization when exposed to air. All fabrication steps used to create the device geometry on the 2DEG wafer are done using electron beam lithography (EBL), wet chemical etching, metallization, and rapid thermal annealing. The fabrication details can be found in Ref. 5.

### C.2. Measurement Methods

Two scanning electron micrographs of the ballistic electron devices used in our experiments are shown in Fig. 1(b-c), labeled as device 1 and 2 respectively from here on. Both figures show the intersection of four leads (terminals), containing an asymmetric (triangular) antidot, a scatterer for electrons. An important property of device 2 is the complete symmetry of the device, except the central triangular scatterer. The electrons in the terminals are heated using two opposing, 180° out of phase, 37 Hz AC currents, $\nu^{\pm}_H$, applied to the individual heating channels. Fig. 1(b-c) show example circuit diagrams for these measurements. The $1\omega$ (37 Hz) voltage at the heated terminal, as measured by the voltage probes $P_1$ and $V_{(1,2,3,4)}$ in the respective devices, is minimized by tuning the relative amplitudes of $\nu^{\pm}_H$. Any DC voltage measured here is also removed by applying a DC shift, $V_{DC}$, to $\nu^{\pm}_H$. The thermovoltage responses are then measured by measuring the voltages at each terminal using the available voltage probes. Using this method, we can measure the thermovoltage response due to heating the electrons in terminals 1 or 3 for the device 1, and any of the four terminals for the device 2. When heating terminal 3 in device 1, however, we cannot minimize the DC and $1\omega$ voltage due to the lack of a side voltage probe.

The junctions' response to an electronic excitation was also measured to characterize their linear and nonlinear transport properties. The electronic measurements were conducted by applying a controlled electric current between two terminals while measuring the voltage responses at each terminal. Due to the geometry of device 1, the device could only be electrically biased between terminals 1 and 3. See Refs. 1, 5, and 7 for additional details on both measurements.

In addition to applying the electrical and thermal biases to device 2, we could also apply a magnetic field perpendicular to the plane of the 2DEG to study the quantum thermoelectric transport symmetries. In addition to the varying electrical and thermal excitation stated above, our symmetry measurements consist of a constant electrical or thermal excitation with a varying magnetic field. For each of these symmetry measurements, multiple four-terminal combinations are used to gather the required information for analyzing the junction's symmetry.
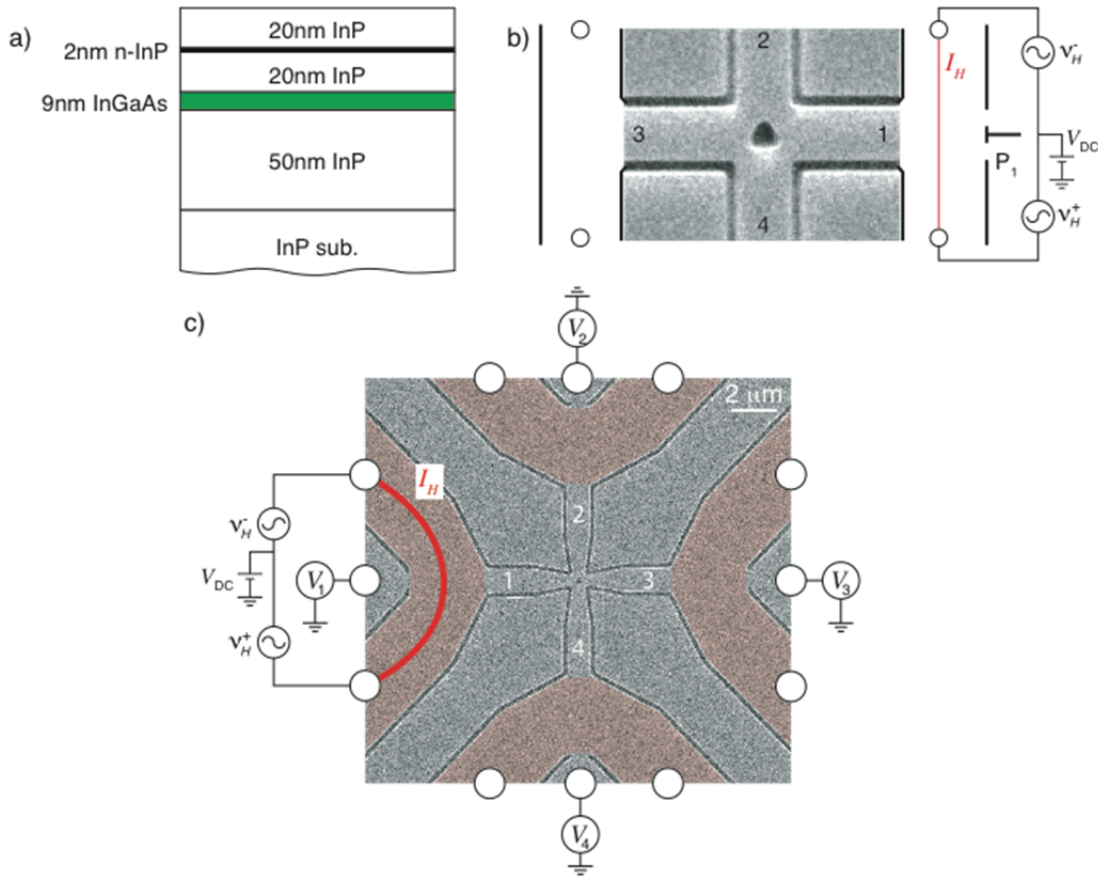


**Fig. 1.** In (a), a cross-section of the heterostructure InGaAs/InP wafer is shown; the dopant layer is depicted by the black band and the 2DEG the green band. In (b), a typical measurement setup for a four-terminal junction is shown around a scanning electron micrograph (SEM) of a junction. In (c), a second device is shown that has been tailored to study the magnetic-field symmetries of quantum thermoelectric transport in these four-terminal junctions. The central junction in (c) is similar in structure and size to the junction shown in (b). In both (b) and (c) the four terminals in the junction are numbered 1 through 4. The white circles on the edges of the two devices indicate the contact points to the side channels, which are used to bias the devices both electrically and thermally. Panel (b) was taken from Ref. 1, and panel (c) was taken from Ref. 7.

## D.  Results and Discussion

### D.1.    Transverse Thermovoltage Response

The key experiment is to apply a heating current to terminal 1, and to measure the transverse voltage response across terminals 2 and 4.  The first four harmonics, with the first being the frequency of the heating voltage, of the transverse thermovoltage show that the 2nd harmonic dominants the transverse response, Fig. 2(a). Since Joule heating generates the temperature increase in the terminal, a dominant 2nd harmonic is indicative of a linear response to the applied temperature differential.

The literature[6] also shows a dominant 2nd harmonic due to electrical excitation. We were able to confirm that the transverse response we observe is due to thermal effects by measuring the lateral voltage drop across the junction during the heating measurements, Fig. 2(a) inset, and comparing it to the junction's response to electrical excitations, Fig. 2(b). We find that the resulting $2\omega$ response due to the lateral voltage drop is around 10 nV, which is roughly 100 times smaller than the observed thermoelectric response.
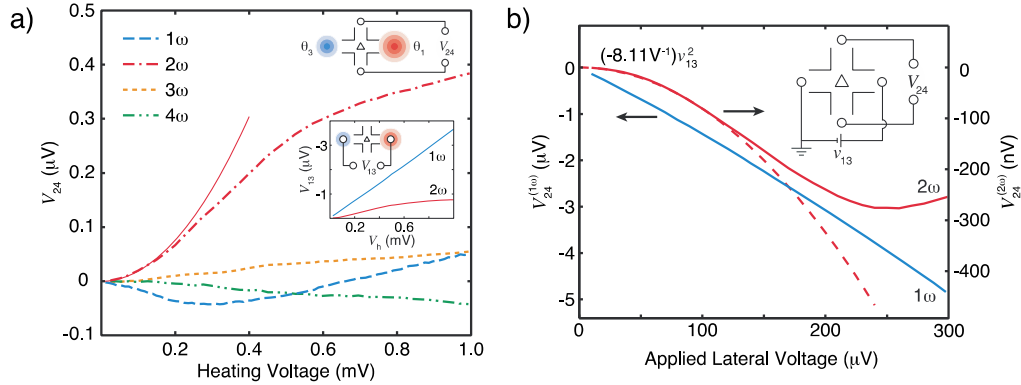


**Fig. 2.** Panel (a) shows the first four harmonics of the transverse thermovoltage. The dominance of the $2\omega$ signal indicates that the response in linear in the applied temperature differential. The inset shows the measured lateral voltage drop during the applied thermal gradient measurements. In panel (b) we checked that the $2\omega$ observed response is not due to electronic excitations by characterizing the junction's electronic response. Figures taken from Ref. 1.

### D.2.    Observed Left-Right Asymmetry and the Two Quantum Point Contact Model

Based on the left-right geometric symmetry of the junction, a naïve guess would say that the transverse thermovoltage should not change upon reversing the lateral thermal gradient, that is, $V_{24}(\theta_1,\theta_3) \approx V_{24}(\theta_3,\theta_1)$. Upon reversing the lateral thermal gradient however, we find that transverse thermovoltage changes sign.

This observation can be understood by conceptually treating the junction as two quantum point contact (QPC) pairs. The thermopowers of the top-right and bottom-right QPCs determine the junction's response to heating terminal 1. Similarly, the thermopowers of the left QPC pair determines the response to heating terminal 3. Since a QPC's thermopower is a series of peaks as a function of the Fermi energy (occupation umber), the sign change in our device can easily arise due to a slight left-right asymmetry in the QPC widths.

The conceptual two QPC model is also able to give a simplistic explanation about the non-linearities in the thermovoltages, indicated by the vertical dashed lines in Fig. 3. As the

6

temperature drop across a QPC increases, its total thermopower increases due to thermal broadening about the Fermi energy accessing neighboring thermopower peaks. The downward change in slope in the heat-right curve can then be interpreted as an increase in the number of accessed thermopower peaks in the top right QPC as a function of $\theta_1$. Similarly for the heat-left configuration, the two nonlinear points indicate increases in the number of accessed thermopower peaks in the bottom left QPC.
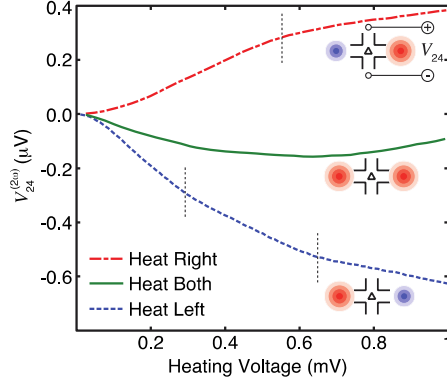


**Fig. 3.** Upon reversing the lateral thermal gradient, we see that the transverse thermovoltage changes sign, something initially unexpected based on the geometrical symmetry of the junction. The vertical dashed lines roughly indicate the onset of the non-linear regions in the transverse responses. Figure taken from Ref. 1.

### D.3.    Multi-Terminal Thermoelectric Scattering Theory

Though the two QPC model is a useful model, all four QPCs in the junction interact with each other, something the two QPC model neglects. To fully treat the four-terminal junction, we developed a multi-terminal scattering theory capable of describing any ballistic, mesoscopic junction up to quadratic order in the voltages and linear order in the temperatures. We found that the current through the $\alpha^{\text{th}}$ junction, $I_\alpha$, can be described as

$$I_\alpha = \sum_\beta \left[ G_{\alpha\beta}\left(V_\alpha - V_\beta\right) + \sum_\gamma \left(V_\alpha - V_\gamma\right)G_{\alpha\beta\gamma}\left(V_\alpha - V_\beta\right) + L_{\alpha\beta}\left(\theta_\alpha - \theta_\beta\right) \right]$$

$$G_{\alpha\beta} = \frac{2e^2}{h}t_{\alpha\beta}(E_F)$$

$$G_{\alpha\beta\gamma} = -\frac{e^3}{h}\left.\frac{\partial t_{\alpha\beta}}{\partial E}\right|_{E_F}\delta_{\beta\gamma} - \frac{2e^2}{h}\left.\frac{\partial t_{\alpha\beta}}{\partial V_\gamma}\right|_{E_F}$$

$$L_{\alpha\beta} = \frac{2\pi^2 e k_B^2 \theta}{3h}\left.\frac{\partial t_{\alpha\beta}}{\partial E}\right|_{E_F}$$

where $e$ is the electron charge, $h$ is Planck's constant, $k_B$ is the Boltzmann constant, $\theta$ is the background temperature, $E_F$ is the common Fermi energy, $t_{\alpha\beta}$ is the transmission probability between the $\alpha^{\text{th}}$ and $\beta^{\text{th}}$ terminals, $V_\alpha$ is the voltage in the $\alpha^{\text{th}}$ terminal, $\theta_\alpha$ is the voltage in the $\alpha^{\text{th}}$ terminal.

Using this scattering theory, we were able to estimate the temperature increase in terminal 1 as a function of the applied heating voltage and thus estimate the effective transverse thermopower of the junction[1]. We found a transverse thermopower of roughly 600 nV/K, which is comparable to the difference between two QPC thermopowers.

### D.4. Magnetic-Field Symmetries in Quantum Thermoelectric Transport

Based on micro-reversibility, the thermoelectric transport properties of our devices should be symmetric under a reversal of the magnetic field if the current and voltage leads are exchanged at the same time. For electrically biased transport, this leads to specific symmetries in the transmission function, $t_{\alpha\beta}(E,B) = t_{\beta\alpha}(E,-B)$, where $t_{\alpha\beta}$ is the transmission function between terminals $\alpha$ and $\beta$, E is the electron energy, and B is the magnetic field. These symmetries have been thoroughly investigated in past literature through measurements using electronic excitation. Since the thermoelectric coefficients, $L_{\alpha\beta}$, are dependent on the energy derivative of the transmission function, $\partial_E t_{\alpha\beta}$, we expect that the same symmetries should be present in the thermally driven case,

$$L_{\alpha\beta}(B) = L_{\beta\alpha}(-B).$$

Our observations show that both the electronic and thermal linear-symmetries are present in our devices, Fig. 4. Figure 4(a) shows two expected symmetries based on the measured four-terminal electrical resistances, $R_{\alpha\beta,\delta\gamma} = V_{\alpha\beta} / I_{\delta\gamma}$, the symmetries of which are $R_{\alpha\beta,\delta\gamma}(B) = R_{\delta\gamma,\alpha\beta}(-B)$. The newly observed thermal bias symmetries are shown in Fig. 4(b-d).

Though the magnetic field traces in Fig. 4 show the expected symmetries, the symmetries are not as perfect as expected. Significant small-scale fluctuations are present in the electric and thermal bias measurements, though smaller in relative magnitude for the former. Two possible explanations for the deviation in the thermal bias measurements are: i) unintentional heating of the three non-heated terminals, for example terminals 2, 3, and 4 in Fig. 1(c); and ii) inelastic scattering of electrons, which has already been shown[8,9] to lead to asymmetries in the thermopower.
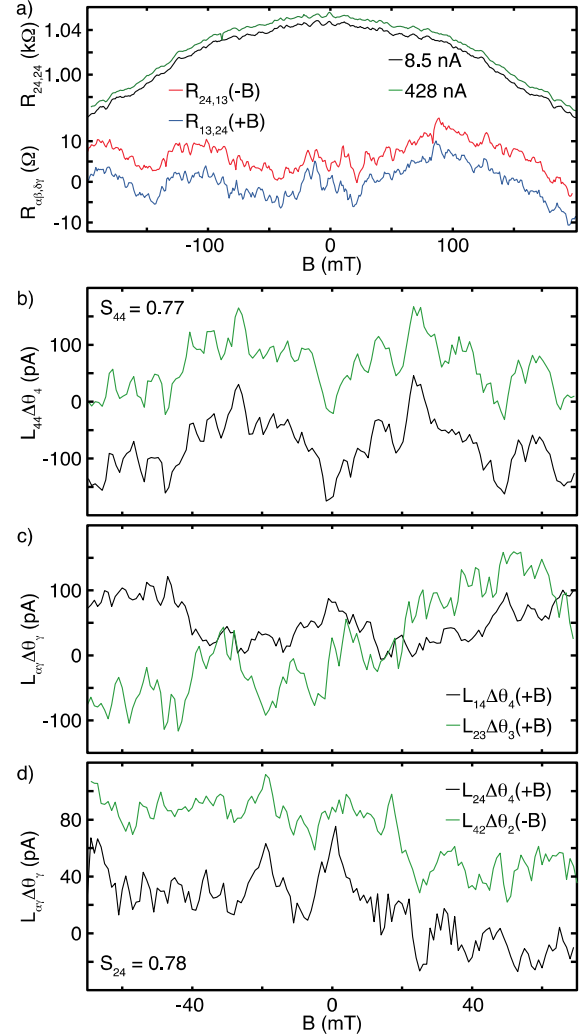


**Fig. 4.** In our device, the well-established magnetic-field symmetries under constant electrical bias are clearly evident, panel (a). The newly observed magnetic-field symmetries under constant thermal bias seen in this work show that the symmetries described by $S_{\alpha\beta}$ hold true. Panels (b) and (d) show expected symmetries. Panel (c) shows two traces that are not expected to be symmetric. The green and red curves in each panel are offset for clarity. Figure taken from Ref. 7.

8

### D.5. Magnetic-Field Symmetries at Finite Thermal Bias

To further study the thermoelectric transport symmetries in these devices, we looked at the magnetic-field symmetries under finite thermal biases, i.e. the non-linear regime. To quantify the degree of symmetry as a function of thermal bias, we introduced the symmetry parameter

$$S_{\alpha\beta} = \sum_B M_{\alpha\beta}(B) M_{\beta\alpha}(-B),$$

where

$$M_{\alpha\beta}(B) \equiv \frac{L_{\alpha\beta}(B) - \langle L_{\alpha\beta}(B) \rangle}{\sqrt{\sum_B \left( L_{\alpha\beta}(B) - \langle L_{\alpha\beta}(B) \rangle \right)^2}}.$$

Note that $S_{\alpha\beta}$ ranges from -1 to +1, were -1 represents complete anti-symmetry, and +1 represents complete symmetry. The results of our symmetry analysis are shown in Fig. 5. We observe that the dominant trend of $S_{\alpha\beta}$ is to decrease with increasing thermal bias. However, this trend is not universal to all of the symmetry parameter's components; a few of the off-diagonal components remain unchanged or even show a slight increase in symmetry with increasing thermal bias. The origin of the decreasing symmetries could be due to non-linear thermoelectric effects, which we estimate to begin at $V_H \sim 1$ mV; however, they could also be due to other effects, such as heating of the non-heated terminals.
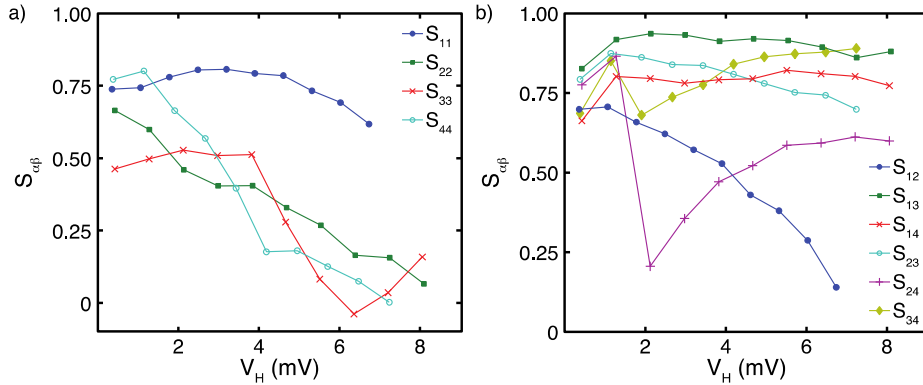


**Fig. 5.** Here we show the symmetry parameter, $S_{\alpha\beta}$, as a function of the applied heating voltage. The diagonal components, $\alpha = \beta$, show a clear decrease as the thermal bias is increased. The same decrease is only partially seen in the off-diagonal components, $\alpha \neq \beta$.

9

E. Conclusions. Our results have shown that the transverse thermopower of the four-terminal junction with a central scatterer is very sensitive to the symmetry of the four QPC transmissions functions. We have shown that as a first order conceptual model, the four-terminal junction can be thought of as two pairs of QPCs, one left and one right. This model is capable of describing both the observed sign change in the transverse thermopower upon reversal of the thermal gradient, as well as the observed nonlinear effects in the transverse thermopowers. To fully take all four terminals into account, we have put forth a multi-terminal thermoelectric scattering theory, which we have used to extract the applied temperature increase as well as the effective transverse thermopower. Finally, we have experimentally demonstrated the fundamental magnetic-field symmetries of thermoelectric transport coefficients under thermal and electrical biases. We have also shown that these symmetries tend to decrease with increasing thermal bias. From our experiments we cannot conclude whether this symmetry breaking is due to a heating effect (for example the destruction of phase coherence due to inelastic scattering) or due to a nonlinear effect.

## F. Ongoing and Future Work

### F.1. Second Generation Devices

In response to the measurements reported in Section D.1-3 and Ref. 1, we fabricated a second generation of devices designed to investigate the symmetry of the four-terminal junctions, Fig. 1(c), a device with a vertically displaced circular scatterer, Fig. 6(b), and arrays of triangular scatterers. The symmetry measurements have been completed and are stated in Section D.4-5

The circular device will test our hypothesis that the exact shape of the scatterer is not critical to generating the observed thermoelectric effects. The multi-terminal scattering theory we have developed, and the electronic and thermal bias measurements on device 2 support this hypothesis. In particular, for the said measurements, we have seen comparable transverse thermovoltages while individually heating each of the four terminals in the device shown in Fig. 1(c). We also have preliminary electronic measurements on the circular scatterer device that suggest this is true, Fig. 7.

Devices consisting of arrays of triangular scatterers were also fabricated. In a possible continuation of this project, these devices will be used to explore transverse thermoelectric effects in a scaled-up functional nanomaterial, Fig. 6(b), as well as whether asymmetric, nanoscale obstacles can be used to partially rectify the flow of heat carried by electrons, Fig. 6(c).
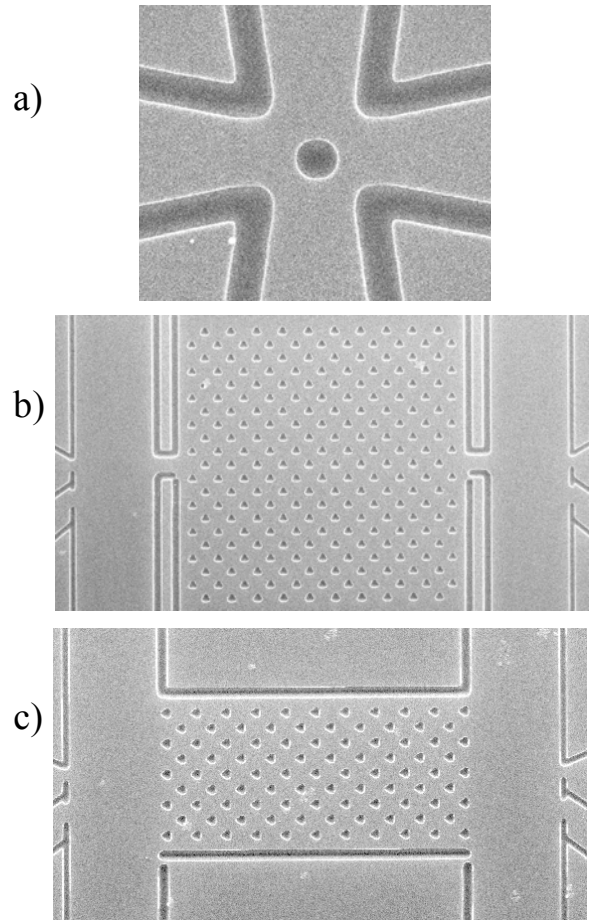
**Fig. 6.** Three of seven new device structures fabricated to test for the rectification of heat flow. (a) Device with a circular central scatterer. (b) Array of triangular scatterers used to test functional nanomaterial properties. (c) Device structure for studying the rectification of heat flow.

10
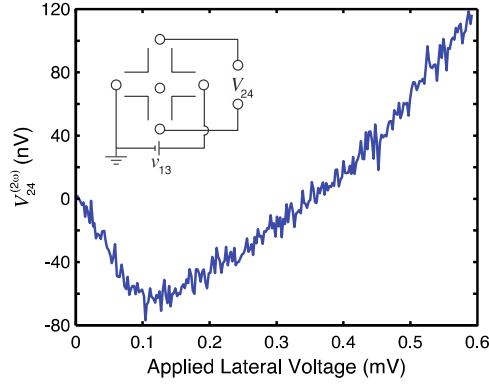
**Fig. 7.** The observed transverse voltage response, $V_{24}$, of the displaced circular scatterer device, Fig. 6(a), due to a lateral electronic excitation suggests that the exact geometrical symmetry of the scatterer is not critical to generating the observed effects. The key point here is that the magnitude of the observed transverse voltage is comparable to that from the device with a triangular scatterer.

### F.2.    Theoretical Analysis

We are collaborating with two theorist groups: David Sanchez, Mallorca and Peter Samuelsson, Lund. Through these collaborations, we are refining the multi-terminal thermoelectric scattering theory described in section D.3. Using this model and the measurements discussed in Section D.3-4., we are actively comparing the observed experimental symmetries with theoretical predictions.

### F.3.    Numerical Simulations

Peter Samuelsson's group is conducting numerical simulations of the symmetry device shown in Fig. 1(c). Their simulations use a recursive Green's function algorithm to model the scattering matrix describing the junction. Due to the sensitivity of the actual device to its dimensions and stray charges, we do not expect to achieve complete agreement between experiments and simulations. Instead, we intend to compare the statistical properties of the junction's transport properties, such as the magnitude of the transverse voltage as a function of an applied magnetic field.

## G. References

1       J. Matthews, D. Sanchez, M. Larsson, and H. Linke, *Thermally driven ballistic rectifier*, Phys. Rev. B **85**, 205309 (2012); arXiv:1107.3179v3 [cond-mat.mes-hall].
2       P. Ramvall, N. Carlsson, P. Omling, L. Samuelson, W. Seifret, M. Stolze, and Q. Wang. Ga0.25in0.75as/inp quantum wells with extremely high and anisotropic two-dimensional electron gas mobilities. Appl. Phys. Lett., **68**(8): 1111 − 1113, February 1996.
3       M. Larsson, D. Wallin, and H. Q. Xu. A highly tunable lateral quantum dot realized in InGaAs/InP by an etching technique. J. Appl. Phys., 103:086101, April 2008.
4       Colleen Marlow. Electronic Quantum Interference in Semiconductor Billards. Ph.D. thesis, University of Oregon, August 2005.
5       Jason Matthews. Thermoelectric and Heat Flow Phenomena in Mesoscopic Systems. Ph.D. thesis, University of Oregon, December 2011.

6       A. M. Song, A. Lorke, A. Kriele, J. P. Kotthaus, W. Wegscheider, and M. Bichler, *Nonlinear electron transport in an asymmetric microjunction: A ballistic rectifier* Physical Review Letters **80**, 3831 (1998).

7       J. Matthews, F. Battista, P. Samuelsson, D. Sanchez, and H. Linke, *Experimental test of magnetic-field symmetries in quantum thermoelectric transport* (near submission)

8       D. Sánchez and L. Serra, Phys Rev. B **84**, 201307(R) (2011).

9       K. Saito, G. Benenti, G. Casati, and T. Prosen, Phys Rev. B **84**, 201306(R) (2011).

## H. List of Symbols, Abbreviations, and Acronyms

2DEG – two-dimensional electron gas

$V_1$, $V_2$, $V_3$, and $V_4$ – the voltages in the four terminals of the junction.

$\theta_1$, $\theta_2$, $\theta_3$, and $\theta_4$ – the temperature rises in the four terminals of the junction.

$e$ – electron charge (defined as a positive quantity)

$h$ – Planck's constant

$k_B$ – Boltzmann constant

$E_F$ – Fermi energy

## I. Project Output

### I.1. Conference presentations

1) "Low-temperature thermoelectric phenomena in nanostructures"
Heiner Linke
Microkelvin Workshop, Smolenice, Slovakia
March 20, 2012 (invited talk)

2) "Nonlinear thermoelectric effects in semiconductor nanostructures"
Symposium on Nanoscale Heat Transfer
Materials Research Society Spring Meeting, San Francisco, USA
April 25-29 (2011) (invited talk)

3) "Fundamental studies of thermoelectric effects in nanostructures"
TD2011: Thermodynamics - can macro learn from nano?
ESF and EOARD sponsored workshop in Snogeholm, Sweden
May 23-25 (2011) (invited talk)

### I.2. Archival papers submitted and status

1.      J. Matthews, D. Sanchez, M. Larsson, and **H. Linke**
"Thermally driven ballistic rectifier"
*Phys. Rev. B 85, 205309 (2012).*

2.      J. Matthews, E.A. Hoffmann, C. Weber, A. Wacker, and **H. Linke**
"Heat flow in InAs/InP heterostructure nanowires"
*Phys. Rev. B 86, 174302 (2012)   DOI: 10.1103/PhysRevB.86.174302*

3.      J. Matthews, F. Barista, D. Sanchez, P. Samuelsson, and **H. Linke**
"Thermoelectric Magnetic-field Symmetries in Ballistic Devices"

*Manuscript, to be submitted to Nature Physics or Physical Review Letters in January 2013.*

**I.3.    Any other publications**

n/a

**I.4.    Patents**

n/a

**I.5.    Any advanced degrees awarded**

Jason Matthews, PhD, University of Oregon, December 2011
Thesis:  *THERMOELECTRIC AND HEAT FLOW PHENOMENA IN MESOSCOPIC SYSTEMS*